Direct Imaging by Cryo-TEM Shows Membrane Break-Up by Phospholipase A_2 Enzymatic Activity†

Thomas H. Callisen* and Yeshayahu Talmon‡

Department of Chemistry, Technical University of Denmark, DK-2800 Lyngby, Denmark, and Department of Chemical Engineering, Technion−Israel Institute of Technology, Haifa 32000, Israel

Received February 2, 1998; Revised Manuscript Received April 22, 1998

ABSTRACT: Phospholipid hydrolysis to free fatty acid and 1-lyso-phospholipid by water-soluble phospholipase A_2 (PLA_2) at the surface of lipid membranes exhibits a poorly understood transition from a low-activity lag phase to a burst regime of rapid hydrolysis. Understanding this kinetic phenomenon may increase our insight into the function of PLA_2 under physiological conditions as well as into general interfacial catalysis. In the present study we apply for the first time cryo-transmission electron microscopy (cryo-TEM) and high-performance liquid chromatography (HPLC) to characterize the PLA_2 hydrolysis of phospholipid vesicles with respect to changes in lipid composition and morphology. Our direct experimental results show that the initial reaction conditions are strongly perturbed during the course of hydrolysis. Most strikingly, cryo-TEM reveals that starting in the lag phase, vesicles become perforated and degrade into open vesicles, bilayer fragments, and micelles. This structural instability extends throughout the system in the activity burst regime. In agreement with earlier reported correlations between initial phospholipase activity and substrate morphology, our results suggest that the lag−burst phenomenon reflects a cascade process. The PLA_2-induced changes in lipid composition transform the morphology which in turn results in an acceleration of the rate of hydrolysis because of a strong coupling between the PLA_2 activity and the morphology of the lipid suspension.

Phospholipase A_2 (PLA_2)[1] embraces a ubiquitous family of enzymes which catalyzes the hydrolysis of phospholipid to 1-acyl-lyso-phospholipid and free fatty acid. These molecular degradation products may have strong impact on the physical stability and organization of the lipid matrix at which the lipolytic reaction takes place, because both hydrolysis products favor nonplanar geometries of the lipid aggregates, that is, normal micelles and inverted hexagonal phases for the lyso-phospholipid and the fatty acid, respectively (*1*). Therefore, our understanding of the function of PLA_2 (and possibly other lipases) in metabolism, immunological response, and digestive reactions among many physiological processes (*2*) may benefit from a detailed physical characterization of the dynamic interplay between PLA_2 activity and lipid organization. Water-soluble PLA_2's are interfacially activated (*3*−*5*); the enzyme activity is strongly enhanced when the substrate is presented in an aggregated state (e.g., micelles and vesicles), as compared to when the substrate is in the monomeric form. Another type of activation is described on the basis of a widely observed transition in the rate of PLA_2 hydrolysis from an initial phase of low activity to a regime of rapid hydrolysis (*6*, *7*). For lipid bilayer substrates, the biophysical studies of this lag−burst hydrolysis reaction have been very extensive. By and large, this system serves as a fairly simple model system for investigating fundamental molecular and thermodynamic effects relevant for interfacial catalysis. The delicate interplay between the PLA_2 activity and the physicochemical properties of lipid bilayers also lends itself as a model system to the study of general physical principles which may affect the regulation of membrane protein activity, for example, caused by molecular segregation processes in the plane of the membrane or due to changes in transmembrane pressure gradients (*1*, *8*−*10*).

Despite the great interest in the PLA_2 hydrolysis reaction, the physical characterization of the lag−burst phenomenon is still incomplete (*1*, *6*, *7*). The variation in PLA_2 activity has been related to changes in affinity of the enzyme for the bilayer surface upon generation of negatively charged fatty acid and to changes in lateral packing properties of the lipid molecules within the bilayers. However, these effects alone do not account for the lag−burst phenomenon. This kinetic scenario prevails for bilayers of negatively charged lipids where all enzyme initially binds (*7*), and at elevated temperatures where the bilayers are in a thermodynamic single-phase region (*1*). We shall discuss here the modulation of the rate of hydrolysis due to a highly nonequilibrium phase transition in the lipid suspension which is driven by the ongoing enzymatic activity. An important experimental

† This work was supported by the Carlsberg Foundation, the Danish Natural Science Research Council (to THC), and the United States−Israel Binational Science Foundation, Jerusalem (to Y.T.).

* Corresponding Author: Department of Chemistry, Building 206, Technical University of Denmark, DK-2800 Lyngby, Denmark. Phone: +45 4525 2440. Fax: +45 4593 4808. E-mail: hoenger@kemi.dtu.dk.

‡ Technion−Israel Institute of Technology.

[1] Abbreviations: PLA_2, phospholipase A_2; DPPC, dipalmitoylphosphatidylcholine; LysoPPC, 1-lyso-palmitoylphosphatidylcholine; PA, palmitic acid; LUV, 100 nm unilamellar vesicles; cryo-TEM, cryo-transmission electron microscopy; HPLC, high-performance liquid chromatography.

S0006-2960(98)00255-4 CCC: $15.00
Published on Web 07/15/1998

task is to clarify the relationship between the PLA_2 activity and the substrate morphology. Previous ^{13}C and ^{31}P NMR spectroscopy studies of the PLA_2 hydrolysis reaction (*11*, *12*) have indicated large-scale morphologic rearrangements during the lag−burst reaction, but an unambiguous microscopic interpretation of these spectroscopic observations has been missing. There has also been a lack of accurate quantitative data on the lipid hydrolysis during lag−burst reactions. PLA_2 activity on the exterior of a vesicle instantaneously causes a migration of protonated fatty acid molecules to the inner leaflet of the vesicle (*13*). Due to the permeability barrier of the lipid bilayer, the fatty acid equilibration process in turn builds up proton gradient between the vesicle lumen and the exterior. This phenomenon obscures the results obtained by the standard pH-stat activity assay for fatty acid release. Notably, pH-stat activity data are the basis for most of the correlations between the PLA_2 activity and physical properties of systems which display lag−burst behavior (*6*, *7*).

In this publication we present results obtained during lag−burst hydrolysis reactions by cryo-TEM direct imaging of the morphology and by HPLC direct quantitation of the lipid composition. Cryo-TEM has previously been applied in the characterization of morphologic transitions, for example, from lamellar to hexagonal phases and from vesicles to micelles (*14*, *15*). Our present work is the first application of cryo-TEM in a study of an enzymatically induced morphologic transition. Although HPLC and combined chromatographic/radioactive assays have been used to quantitate PLA_2 activity (*16*, *17*), the lag−burst hydrolysis reaction has not been characterized by direct quantitative methods.

MATERIALS AND METHODS

Dipalmitoylphosphatidylcholine (DPPC) as powder is purchased from Avanti Polar Lipids. Purity is checked by HPLC as outlined below. The monomeric aspartate-49 isomer of PLA_2 from the venom of *Agkistrodon piscivorus piscivorus* is obtained from Sigma Chemical Co. and purified according to Maraganore et al. (1984) (*18*). PLA_2 concentrations are determined by absorbance at 280 nm, using an extinction coefficient of 2.2 mL/mg/cm. One-component 100 nm unilamellar vesicles (LUV) are prepared by extrusion through 100 nm polycarbonate filters with a device from Lipex Biomembranes Inc. (*19*). The LUVs are examined by cryo-TEM as explained below. All lipid suspensions are thermally equilibrated for at least 1 h prior to experiments. The buffer contains 150 mM KCl, 1 mM NaN_3, 30 μM $CaCl_2$, 10 μM EDTA, and 10 mM Hepes (pH 8). The choice of salt concentrations in this buffer prevents extensive calcium-palmitate precipitation (*20*), and minimizes changes in the concentration of the cofactor Ca^{2+} at the vesicle surface upon formation of negatively charged fatty acid (*21*). As a common reference experiment for the extraction of samples to HPLC and cryo-TEM, we monitor the PLA_2 intrinsic fluorescence intensity at 340 nm upon excitation at 285 nm using an SLM Aminco 8100 spectrofluorometer (*22*). The PLA_2 intrinsic fluorescence displays a very reproducible and systematic variation during lag−burst reactions, for example, as a function of reaction temperature and lipid chain length (*23*). A physical interpretation of these variations is, nevertheless, complicated by the fact that numerous physical events during the hydrolysis time course may affect the fluorescence intensity (*6*, *11*). This type of data will be discussed elsewhere in relation to NMR experiments (Callisen et al., manuscript in preparation).

High-Performance Liquid Chromatography. HPLC quantitation is made on a Waters Millenium 2010 system equipped with a Waters 510 pump, a Waters 717 Plus autosampler, and a PL-EMD 950 evaporative light-scattering mass detector from Polymer Laboratories. We use a 5 μm Phenomenex diol spherical column and a mixture of chloroform/methanol/water/acetic acid (730:230:25:0.1, v/v) as an isocratic mobile phase. Retention times are 5.1 min for palmitic acid (PA), 7.4 min for DPPC, and 21.5 min for 1-lyso-palmitoylphosphatidylcholine (LysoPPC). Lipid extractions (45 μL) are made simultaneously with the collection of intrinsic enzyme fluorescence from reactions in the spectrofluorometer with 2.5 mM DPPC LUV and 1.0 μM PLA_2. The extracted samples are rapidly mixed in chloroform/methanol arriving at the composition of the mobile phase (without acetic acid). The effectiveness of this quench procedure was assessed by adding 10 mM EDTA to a reaction at different points during the lag−burst time course. We see no systematic deviation in area of the substrate component of extractions before and at different time points after the EDTA quench. Our quantitative analysis is a relative measure of the degree of hydrolysis, that is, we analyze the reduction in the substrate fraction of the lipid extractions. DPPC dose/response calibration curves of the HPLC system are linear well beyond the concentration range examined.

Cryo-Transmission Electron Microscopy. Lipid suspensions (15 mM) for cryo-TEM are thermally equilibrated in the temperature- and humidity-controlled environment vitrification system (CEVS) (24). For the time-resolved studies of the PLA_2 reactions, 1.5 μM PLA_2 is mixed with the lipid suspension to initiate hydrolysis. Prior to these microscopy experiments, the lag times are estimated from the analogous experiments in the spectrofluorometer, as described above, with and without stirring but under otherwise identical conditions. Independently of stirring we observe distinct lag phases, although the evolution of the PLA_2 fluorescence intensity signal indicates a less abrupt crossover from a lag to a burst regime in the absence of continuous stirring. Vitreous cryo-TEM specimens are produced as a function of the reaction time in effect making our technique "time-resolved cryo-TEM", as demonstrated before (*14*, *25*). Specimens are prepared by applying a drop, ~5 μL, of the lipid suspension onto a perforated carbon film covered TEM copper grid, held by a tweezer inside the CEVS. The drop is then blotted to the right thickness of approximately 0.3 μm and plunged into a reservoir of liquid ethane at its freezing point. This procedure ensures preservation of the microstructure in the liquid phase as well as in the thermally fixed specimen, which is vitrified due to the very high cooling rate, higher than 100 000 K/s (*25*). The vitrified specimen is transferred by an Oxford CT3500 cooling-holder into a Philips CM120 BioTwin cryo-TEM, where they are kept at about −170 °C. We image the specimens with 120 kV electrons by a Gatan 791 cooled multiscan CCD camera, at a microscope original magnification of 33 000 times using a low electron-dose procedure to minimize electron beam radiation damage. The application of digital imaging pro-

vided immediate feedback for assessment of the results and easy post-microscopy image processing, especially background subtraction to enhance image contrast.

For the present purpose, cryo-TEM is superior to other microscopic techniques because the rapid thermal quench of the reacting lipid suspension effectively traps the momentary state of the system with respect to enzyme activity and morphology. Moreover, the direct imaging in cryo-TEM is free of possible artifacts introduced by a staining protocol (*26*). If special precautions are not taken to arrest and preserve the state of this highly labile system, microscopic data will at best give very limited information (*27*). Cryo-TEM has been recently discussed in detail including technical procedures and considerations, as well as issues pertaining to its applicability, advantages, and shortcomings (*28*). This technique is an excellent tool for elucidating the microstructural features of the system, down to the nanometer scale, and through that it provides the physical model usually needed for the interpretation of other sources of data, for examples, from NMR experiments. However, it cannot be considered on its own as a quantitative technique, due to problems of magnification calibration and size segregation during specimen preparation.

RESULTS AND DISCUSSION

The lag−burst phenomenon in PLA_2 hydrolysis of phospholipid vesicles is typically observed in the case of saturated zwitterionic phosphatidylcholines of varying lipid chain length and vesicle size (*23*, *29*), as well as for negatively charged vesicles of phosphatidylglycerol (*30*). With LUVs we analyze here the PLA_2 hydrolysis of DPPC to LysoPPC and PA in discrete time steps by means of HPLC. Figure 1, parts A and B, shows analogous PLA_2 reaction time course experiments at 38 and 47 °C with the DPPC bilayer substrate in the gel and in the fluid phase, respectively. The HPLC data points in Figure 1A indicate an initial fast hydrolysis, succeeded by a regime of lower activity, denoted as the lag phase or the pre-steady-state (*29*). For the fluid phase reaction in Figure 1B, the initial activity and the lag-phase activity appear to be of the same magnitude. It is possible to estimate the enzyme activity in the lag phase from the slope of the hydrolysis versus time curves in Figure 1. Hydrolysis in the lag phase with the gel-phase substrate proceeds at a rate of 0.2 mmol of DPPC/min/g of PLA_2, while a rate of 0.8 mmol of DPPC/min/g of PLA_2 is observed for the fluid-phase reaction.

The lag phase is terminated by acceleration of the hydrolysis reaction; a characteristic lag time defines the time until maximum rate of hydrolysis (*29*). Given the time resolution of the HPLC data in Figure 1, the inflection points in the hydrolysis curves are near 8 and 13 mol % hydrolysis for the gel and fluid-phase reactions, respectively. Maximum enzyme activity occurs after more than 12 mol % of the available substrate has been hydrolyzed at both reaction temperatures. In the activity burst region, the maximum rate of hydrolysis is higher for the fluid than for the gel-phase DPPC LUV reaction, as also seen for the lag-phase activities. From Figure 1 we find an activity of 21 mmol of DPPC/min/g of PLA_2 for the fluid phase system, whereas 8.6 mmol of DPPC/min/g of PLA_2 is found with the gel-state DPPC LUV. For the systems in Figure 1, and for other vesicular

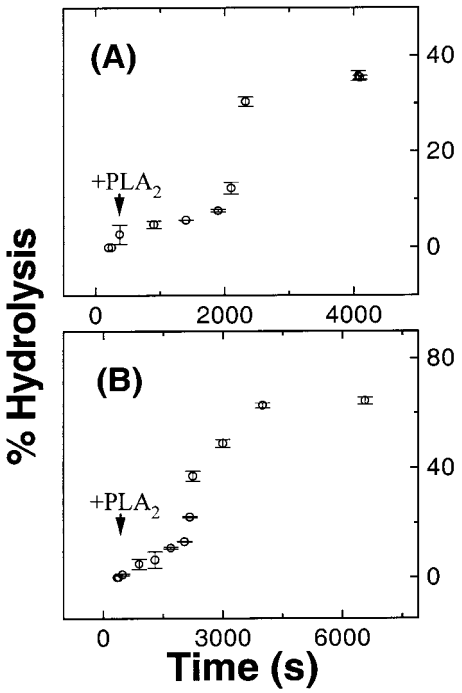

FIGURE 1: Hydrolysis time course experiments conducted at 38 °C (A) and 47 °C (B) for the PLA_2-catalyzed hydrolysis of dipalmitoylphosphatidylcholine (DPPC) provided as 100 nm unilamellar vesicles (LUV). The fraction of hydrolysis is quantified stepwise by high-performance liquid chromatography (HPLC) analysis of the relative reduction in the DPPC signal and is reported as the mean value (open circles) of two HPLC runs of the lipid extractions. The error bars indicate the difference between the DPPC signals in the two runs. Indicated by the arrow, the hydrolysis reaction is initiated by adding PLA_2 to the equilibrated vesicle suspension. The hydrolysis processes display a characteristic transition from a low-activity lag phase to a burst regime of rapid hydrolysis. Conditions: 2.5 mM DPPC LUV and 1.0 μM PLA_2 in a buffer containing 150 mM KCl, 1 mM NaN_3, 30 μM $CaCl_2$, 10 μM EDTA, and 10 mM Hepes (pH 8).

substrates of saturated phosphatidylcholines (*1*, *16*, *17*, *31*), the fraction of conversion at late time stages correlates strongly with reaction parameters such as temperature and Ca^{2+} concentration. When the experiments in Figure 1 are terminated, 65% of the substrate is hydrolyzed in the fluid-phase reaction, while the gel-phase time course has a 35% conversion of the available substrate.

Hitherto, the quantitative analysis of the lag−burst kinetics has been documented only indirectly by pH-stat titration of the fatty acid release (*6*, *7*, *29*, *30*). At variance with our results, the pH-stat generally reports less than 5% hydrolysis prior to the activity burst. The lower level of lag-phase activity reported by the pH-stat originates primarily from method-dependent problems with the titration assay. One problem relates to inaccurate assumptions about the apparent fatty acid pK_a which is very sensitive to the microelectrostatic environment (*32*). Lateral segregation and partitioning of the fatty acid into other mesophases will affect the apparent pK_a. Another obstacle is due to the lipid bilayer permeability barrier. As mentioned earlier, the PLA_2 activity on the exterior of the vesicles results in instantaneous migration of protonated fatty acid molecules to the inner leaflet of the LUVs (*13*). The inefficient detection of protons released to the lumen of the vesicles will offset the pH-stat activity data both in magnitude and in time and thus confuse correlations of the enzyme activity with physical changes in the system.

The PLA_2-catalyzed lipid hydrolysis radically affects the stability of various types of lipid bilayer substrates (*1*, *20*, *31*, *33*−*35*). We had tried to resolve the structural changes in connection with the lag−burst phenomenon for vesicular substrates by means of freeze-fracture electron microscopy (*11*, *12*). To mimic different stages in the lag−burst reaction we investigated the morphology of extensively hydrolyzed LUV preparations from mixtures of DPPC and the unhydrolyzable ether analogue di-hexadecyl-phosphatidylcholine. With increasing amounts of DPPC in the LUV preparation, we observed a growing population of smaller aggregates in coexistence with large bilayer sheets after incubation with PLA_2. Although our spectroscopic experiments were consistent with the formation of mesophases of high curvature, we had no direct evidence for the nature of the dynamic structural rearrangements during the time course of the reaction. For this purpose we have invoked cryo-TEM which previously has been applied in the characterization of the transitions from lamellar to hexagonal phases and from vesicles to micelles (*14*, *15*).

Figure 2A shows gel-phase DPPC LUVs thermally fixed from 40 °C. The extruded lipid suspension is a population of single and oligo-lamellar vesicles of an average nominal size near 100 nm. The faceted surfaces of the vesicles indicate that the bilayers are in the rippled gel phase, denoted $P_{\beta'}$. This micrograph depicts an area near the edge of a hole in the support film. The vitreous ice in this case has a negative thickness gradient from the bottom of the field of view, up. The crowding of the vesicles near the hole edge is a result of specimen preparation and, as noted earlier, does not reflect the bulk concentration.

Figure 2B−D shows micrographs corresponding to three time points in a PLA_2 reaction time course at 47 °C, with the vesicular preparation shown in Figure 2A. In these micrographs the contours of the vesicles are rounded, typical of the fluid L_α phase. This is true also when the vesicles are partially destroyed by the effect of lipid hydrolysis. The lag time in this experiment was estimated on the basis of the characteristic shift in PLA_2 intrinsic fluorescence at the crossover from the lag to the burst regime, see Materials and Methods.

Figure 2B is a cryo-TEM image of a vitrified specimen after 60 s of hydrolysis, supposedly in the lag phase. Two distinct vesicle populations are seen: vesicles of the initial size distribution and much smaller vesicles down to about 20 nm in diameter. Open vesicles, that is, vesicles with missing portions of the bilayer (arrowhead), and bilayer fragments viewed edge-on (arrow) and face-on (thin arrow), are also observed. In cryo-TEM the optical density of noncrystalline objects is related to the density multiplied by the thickness of the object traversed by the electron beam ("mass-thickness"). Thus, an edge-on view of a bilayer fragment is a dense line, while a face-on view of such an object gives a uniform shadow, slightly darker than the background area. Typically vesicles will be seen as dense rings in projection. If a defect is positioned in the perimeter of the vesicle with respect to the incident electron beam, it is easily visible in projection. On the other hand, if the defect is inside the projected areas it will be barely visible, due to low contrast. The structural changes seen in Figure 2B as compared to Figure 2A cannot be ascribed to an instability of the vesicles by the mere physical interaction with the enzyme. In fact, such microstructural changes are typical of membrane solubilization by a surfactant (*15*). In our preliminary cryo-TEM studies which included reactions with very long lag times, we did not observe any structural changes in the vesicle suspension upon prolonged incubation with PLA_2. As stressed earlier, however, an inspection by cryo-TEM would not provide a full quantitative answer to this issue. Instead time-resolved ^{13}C and ^{31}P NMR spectroscopy experiments of lag−burst reactions with DPPC LUVs (Callisen et al., manuscript in preparation) have been performed (*11*). Consistent with our cryo-TEM experiments, the spectral features of the initial ^{13}C and ^{31}P NMR signals from the LUVs remain constant for hours in reactions where the lag phases last more than 10 hours (due to low calcium concentrations).

In Figure 2C the vesicle suspension was incubated for 300 s with PLA_2 which should correspond to a time point in the transition region from slow to fast hydrolysis. Compared with the preceding time point, this micrograph is dominated by open structures (arrowheads) and bilayer fragments (arrows). Large-scale bilayer sheets are also visible in specimens such as the one in Figure 2C. Those appear as larger areas of higher optical density (lower part of the micrograph). At this point in time one can also see small globular micelles (granular background of the micrograph). The vesicles seem to have undergone lysis producing structures similar to the intermediate structures observed in the vesicle-to-micelle transition in detergent−lipid systems (*15*). The final time point at 900 s reaction time represents the system after extensive hydrolysis where activity ceases (Figure 2D). Here micellar aggregates coexist with bilayer sheets and remnant vesicles.

The temporal evolution of the PLA_2 hydrolysis reaction depends critically on reaction conditions, for example, lipid-to-enzyme ratio, calcium concentration, and phase state of the lipid substrate. A variation of the stirring conditions also modulates the lag time of an experiment as seen in Figures 1B and 2 where the PLA_2/DPPC ratios furthermore differ by a factor of 4. However, for the present discussion of the lag−burst phenomenon, it should be noted that the underlying mechanism behind this kinetic phenomenon is conserved within a broad window of these parameters (*7*, *29*). We shall therefore comment on some of the general features of the lag−burst phenomenon in PLA_2 hydrolysis time courses, accentuated by the direct quantitative and structural results provided in Figures 1 and 2.

From a thermodynamic point of view it is frequently claimed (*6*, *7*) that lipid vesicles are stable toward PLA_2-induced conversion because equimolar mixtures of LysoPPC and PA may form a lamellar mesophase (*36*). The phase behavior of ternary dispersions of di-acyl-phospholipids and their PLA_2 hydrolysis products are, however, only partially understood; so far both lamellar and isotropic phases have been observed (*36*−*38*). Recent cryo-TEM and X-ray scattering experiments (Lemmich et al., manuscript in preparation) have shown that the mesophases in these lipid suspensions include nonvesicular structures, even in systems corresponding to 10 mol % hydrolysis. Still, simple ternary mixtures of substrate and PLA_2 products are frequently used to mimic the dynamic system undergoing hydrolysis, with the assumption that only vesicles are formed in these dispersions (*6*, *7*, *29*, *39*).

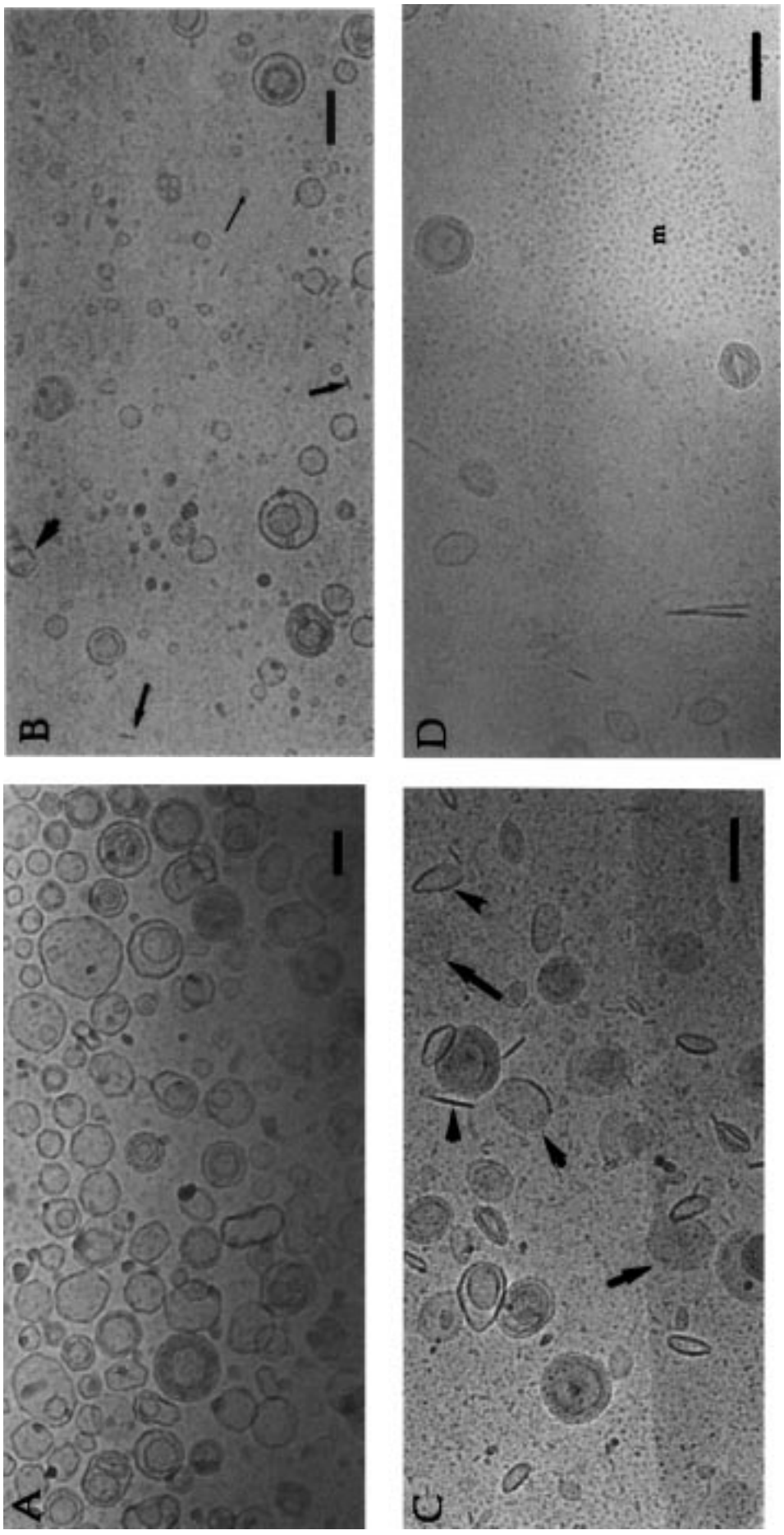

FIGURE 2: Cryo-transmission electron microscopy (cryo-TEM) during the PLA_2-catalyzed hydrolysis of 15 mM DPPC LUV suspensions in the same buffer as in Figure 1. (A) a micrograph of pure DPPC LUV vitrified from 40 °C. The LUV suspension contains single and oligolamellar vesicles of an average nominal size near 100 nm. (B−D) micrographs corresponding to three time points in a PLA_2 reaction time course at 47 °C, with the LUV preparation shown in A. PLA_2 (1.5 μM) is mixed with the lipid suspension to initiate hydrolysis. The lag time in this experiment is estimated from the identical experiment conducted in the spectrofluorometer but without constant stirring. After 60 s of hydrolysis (B), supposedly in the lag phase, the initial vesicle population has shifted toward smaller unilamellar vesicles. Open vesicles (arrowhead) and bilayer fragments seen edge-on (arrow) and face-on (thin arrow) are also seen. In C the LUV suspension has been incubated for 300 s with PLA_2. According to the identical spectrofluorometric reference experiment this point should be in the transition region from slow to fast hydrolysis. Note the abundance of open vesicle structures (arrowhead), bilayer fragments (single arrow) and large-scale bilayer sheets. (D) After 900 s reaction time; represents the system after extensive hydrolysis. Here micellar aggregates (as seen in the region of the letter m) coexist with bilayer sheets and remnant vesicles. Micelles are in some regions excluded from thin vitreous ice domains. Scale bar is 100 nm.

In addition to these equilibrium considerations, it is important to recognize that the PLA_2 activity can induce energetic changes within a single vesicle leading to a structural instability of the individual vesicle at a lipid composition which may differ for the expected equilibrium phase behavior of the suspension (*1*, *9*). First of all, the PLA_2 activity on the exterior of a vesicle alters the spontaneous curvature of the lipid bilayer due to the asymmetric change in molecular composition of the two constituting monolayers of the vesicle. Second, the physical stability of the vesicle may be modified by a coupling between the local lipid composition and the local curvature of the bilayer. Budding and fission processes may be initiated by such types of couplings, for example, from a local enrichment of LysoPPC on the outer monolayer and PA segregation in the corresponding region of the inner monolayer of a vesicle. Our present dynamic results on the PLA_2 reaction, combined with the knowledge about the equilibrium physical behavior of these lipid suspensions, therefore indicate that metastability of the system plays a crucial role in a number of experiments where vesicles remain intact upon extensive hydrolysis (*6*, *7*). It is well-known that curvature and thermotropic phase state of the vesicles modulate the susceptibility of vesicles to undergo structural changes (*40*).

Our HPLC and cryo-TEM results indicate that the regime of extensive vesicle degradation correlates in time with the activity burst region. Indeed, this picture is corroborated by time-resolved ^{13}C and ^{31}P NMR spectroscopy studies of this system and by phase-contrast light microscopy video recordings of the PLA_2 hydrolysis of micron-size unilamellar vesicles (Callisen et al., manuscript in preparation). Several other experimental observations suggest an intimate relationship between the structural instability of the vesicles and the increase in rate of hydrolysis. The maximum rate of hydrolysis for PLA_2 is observed with mixtures of substrate and products corresponding to more than 10 mol % hydrolysis (which yield the nonvesicular mesophases discussed above), and the addition of the hydrolysis products exogenously can trigger spontaneous high activity (*29*). These joint observations lead us to suggest that the lag−burst activity phenomenon reflects a chain-reaction-like process (*11*). The PLA_2-induced lysis of vesicles in our experimental system causes partitioning of hydrolysis products into other vesicles and formation of other mesophases. This dynamic morphologic state of the system in turn is liable to undergo rapid hydrolysis. Heterogeneities in vesicle size and in the distribution of products and enzyme will affect the cooperativity of such a cascade process (*6*).

The correlation between our quantitative results on rate of hydrolysis in Figure 1 and morphology in Figure 2 offers in a simple way an explanation for the changes in the enzymatic activity. During the lag phase, when vesicles are the prominent type of lipid aggregates, we observe a significant temperature dependence of PLA_2 activity. The lag-phase activity in the reaction with fluid-phase LUVs is four times higher than with the gel-phase LUVs. The different dynamic physical properties of the lipid bilayer in the two phases are expected to modulate the rate of hydrolysis via the phase dependence of, for example, the lateral diffusion and the substrate/product exchange dynamics (*1*, *41*). In the activity burst region the hydrolysis rate curiously only differs by a factor of 2.4, suggesting more similar reaction conditions at this stage of the reaction when open vesicles, bilayer fragments, and micelles presumably are more abundant. In previous indirect studies, the burst phenomenon has been ascribed to changes in the organization of the lipids in the plane of the bilayer and in the interaction of the enzyme with the bilayer surface (*6*, *7*). Even though these effects are likely to modulate the PLA_2 activity, their direct contributions to the lag−burst phenomenon have not been established. Our results suggest a simple connection between enzyme activity and morphology of the lipid suspension which explains the lag−burst phenomenon in our system. This interpretation is consistent with earlier comparative studies of phospholipase activity using substrates presented in the form of micelles, vesicles, and hexagonal structures (*16*, *42*). Indeed, a 26−43 times increase in activity when going from the lag phase to the burst regime (as found in Figure 1) might be explained by a change in morphology from a vesicular to a nonvesicular lipid medium. The evolution of nonvesicular mesophases greatly affects the molecular basis for substrate/product exchange as well as product inhibition (*3*−*5*).

In conclusion, the direct experimental results in this paper by cryo-TEM and HPLC provide the basis for a simplified picture of the PLA_2 lag−burst hydrolysis kinetics which relates the enzyme activity to the substrate/product morphology. Further investigations of the dynamic interplay between the PLA_2 activity and the physical properties of the lipid suspensions as well as theoretical modeling are needed to clarify the molecular detail of our results. Other proteins interacting with a structured lipid environment may be affected by perturbations of the physical properties of the lipid organization (*1*, *8*−*10*). Enzymes which directly modify the lipid composition are obvious candidates for this (*42*, *43*).

ACKNOWLEDGMENT

We are grateful to Ms. G. Karlsson for the able help while we performed the cryo-TEM work at the Biomicroscopy Unit at Lund University (Sweden). Thanks are due to Ms. J. Klausen and Dr. K. Jørgensen for assistance with the HPLC experiments. We furthermore thank Dr. R. L. Biltonen for the gift of purified PLA_2 and Drs. R. Verger, O. G. Mouritsen, and L. Miao for helpful criticism of the manuscript. Many stimulating discussions with people in the groups of Biltonen and Mouritsen are appreciated.

REFERENCES

1. Hønger, T., Jørgensen, K., Stokes, D., Biltonen, R. L., and Mouritsen, O. G. (1997) *Methods Enzymol. 286*, 168−190.
2. Kudo, I., Murakami, M., Hara, S., and Inoue, K. (1993), *Biochim. Biophys. Acta 117*, 217−231.
3. Panaiotov, I., Ivanova, M., and Verger, R. (1997) *Curr. Opin. Colloid Interface Sci. 2*, 517−525.
4. Scott, D. L., White, S. P., Otwinowski, Z., Yuan, W., Gelb, M. H., and Sigler, P. B. (1990) *Science 250*, 1541−1546.
5. Nelsestuen, G. L., and Martinez, M. B. (1997) *Biochemistry 36*, 9081−9086.
6. Jain, M. K., Gelb, M. H., and Berg, O. G. (1995) *Methods Enzymol. 249*, 567−614.
7. Burack, W. R., and Biltonen, R. L. (1994) *Chem. Phys. Lipids 73*, 209−222.
8. Gruner, S. M., and Shyamsunder, E. (1991) *Ann. N.Y. Acad. Sci. 625*, 685−697.

9. Sackmann, E. (1994) *FEBS Lett. 346*, 3−16.
10. Cantor, R. S. (1997) *Biochemistry 36*, 2339−2344.
11. Hønger, T. (1994) Ph.D. Thesis, The Technical University of Denmark.
12. Hønger, T., Dibble, A. R. G., Burack, W. R., Allietta, M. M., and Biltonen, R. L. (1995) *Biophys. J. 68*, a464.
13. Kamp, F., and Hamilton, J. A. (1993) *Biochemistry 32*, 11074−11085.
14. Siegel, D. P., Burns, J. L., Chestnut, M. H., and Talmon, Y. (1989) *Biophys. J. 56*, 161−169.
15. Walter, A., Vinson, P. K., Kaplun, A., and Talmon, Y. (1991) *Biophys. J. 60*, 1315−1325.
16. Kensil, C. R., and Dennis, E. A. (1979) *J. Biol. Chem. 254*, 5843−5848.
17. Kupferberg, J. P., Yokoyama, S., and Kèzdy, F. J. (1981) *J. Biol. Chem. 256*, 6274−6281.
18. Maraganore, J. M., Merutka, G. M., Cho, W., Welches, W., Kèzdy, F. J., and Heinrikson, R. L. (1984) *J. Biol. Chem. 259*, 13839−13843.
19. Hope, M. J., Bally, M. B., Webb, G., and Cullis, P. R. (1985) *Biochim. Biophys. Acta 812*, 55−65.
20. Gheriani-Gruszka, N., Almog, S., Biltonen, R. L., and Lichtenberg, D. (1988) *J. Biol. Chem. 263*, 11808−11813.
21. Fernández, M. S., Mejia, R., Zavala, E., and Pacheco, F. (1991) *Biochem. Cell Biol. 69*, 722−727.
22. Bell, J. D., and Biltonen, R. L. (1989) *J. Biol. Chem. 264*, 225−230.
23. Hønger, T., Jørgensen, K., Biltonen, R. L., and Mouritsen, O. G. (1996) *Biochemistry 35*, 9003−9006.
24. Bellare, J. R., Davis, H. T., Scriven, L. E., and Talmon, Y. (1988) *J. Electron Microsc. Tech. 10*, 87−111.
25. Siegel, D. P., Green, W. J., and Talmon, Y. (1994) *Biophys. J. 66*, 402−414.
26. Talmon, Y. (1983) *J. Colloid Interface Sci. 93*, 366−382.
27. Burack, W. R., Dibble, A. R. G., Allietta, M. M., and Biltonen, R. L. (1997) *Biochemistry 36*, 10551−10557.
28. Talmon, Y. (1996) *Ber. Bunsen-Ges. Phys. Chem. 100*, 364−372.
29. Apitz-Castro, R., Jain, M. K., and de Haas, G. H. (1982) *Biochim. Biophys. Acta 688*, 349−356.
30. Burack, W. R., Gadd, M., and Biltonen, R. L. (1995) *Biochemistry 34*, 14819−14828.
31. Hønger, T., and Høyrup, P. (1997) *Eur. Biophys. J. 26*, a72.
32. Cevc, G. (1990) *Biochim. Biophys. Acta 1031−1033*, 311−382.
33. Speijer, H., Giesen, P. L. A., Zwaal, R. F. A., Hack, C. E., and Hermens, W. Th. (1996) *Biophys. J. 70*, 2239−2247.
34. Carlson, P. A., Gelb, M. H., and Yager, P. (1997) *Biophys. J. 73*, 230−238.
35. Alix, S. N., and Woodbury, D. J. (1997) *Biophys. J. 72*, 247−253.
36. Jain, M. K., van Echteld, C. J. A., Ramirez, F., de Gier, J., de Haas, G. H., and van Deenen, L. L. M. (1980) *Nature 284*, 486-487.
37. Allegrini, P. R., van Scharrenburg, G., de Haas, G. H., and Seelig, J. (1983) *Biochim. Biophys. Acta 731*, 448−455.
38. Brentel, I., Arvidson, G., and Lindblom, G. (1987) *Biochim. Biophys. Acta 904*, 401−404.
39. Bell, J. D., Baker, M. L., Bent, E. D., Ashton, R. W., Hemming, D. J. B., and Hansen, L. D. (1995) *Biochemistry 34*, 11551−11560.
40. Mui, B. L.-S., Cullis, P. R., Evans, E. A., and Madden, T. D. (1993) *Biophys. J. 64*, 443−453.
41. Gabriel, N. E., Agman, N. V., and Roberts, M. F. (1987) *Biochemistry 26*, 7409−7418.
42. Robinson, M., and Waite, M. (1983) *J. Biol. Chem. 258*, 14372−14378.
43. Basáñez, G., Nieva, J.-L, Goñi, F. M., and Alonso, A. (1996) *Biochemistry 35*, 15183−15187.

BI980255D